JOURNAL OF MATERIALS SCIENCE 20 (1985) 2103–2109

Enhancement of ionic conduction in CaF_2 and BaF_2 by dispersion of Al_2O_3

SATORU FUJITSU, MASARU MIYAYAMA, KUNIHITO KOUMOTO, HIROAKI YANAGIDA
Department of Industrial Chemistry, Faculty of Engineering, University of Tokyo, Hongo Bunkyo-ku, Tokyo, 113 Japan

TAKAFUMI KANAZAWA
Department of Industrial Chemistry, Faculty of Technology, Tokyo Metropolitan University, Fukasawa Setagaya-ku, Tokyo, 158 Japan

Ionic conductivity measurements were performed on polycrystalline CaF_2, BaF_2 and those dispersed with Al_2O_3 particles. The ionic conductivity of both CaF_2 and BaF_2 increased by about 1 to 2 orders of magnitude by dispersion of Al_2O_3 particles, while X-ray diffraction measurements showed there were no other phases present other than fluoride and Al_2O_3. The conductivity of the dispersed system strongly depended on the particle size and the concentration of Al_2O_3, which suggested the high ionic-conductivity layers were formed at the interface between the ionic conductor matrix and the Al_2O_3 particles. The effective thickness and electrical conductivity of the interface layer at 500° C were calculated, using a simple mixing model, to be 0.3 to ~ 0.6 μm and ~ 10^{-3} S cm^{-1}, respectively.

1. Introduction

Liang [1, 2] found that LiI dispersed with Al_2O_3 particles has larger Li^+ conductivity than the nominally pure LiI, which was supposed to be due to the formation of the high ionic-conductivity layers surrounding Al_2O_3 particles. This type of conductor is different from conventional ones in that heterogeneous interfaces are utilized to give rise to high ionic conductivity. Stoneham *et al.* [3] interpeted morphologically the existence of the interface layer by an effective medium model [4]. Pack *et al.* [5] pointed out that water played an important role for ionic conduction through the interface.

Jow and Wagner [6], and Shahi and Wagner [7] reported similar effects of the Al_2O_3 dispersion in CuCl and AgI, respectively. They proposed the model that the defect concentration and hence the conductivity in the vicinity of the dispersoid (Al_2O_3) were different from those of the bulk of the matrix (conductor) due to the charged double layer formed at the dispersoid/matrix interface. This model could semiquantitatively explain the increase in conductivity with an increasing amount of dispersed Al_2O_3. However, the amount of Al_2O_3 to give a maximum conductivity, its particle size dependence and the thickness of a high conductivity layer still remain to be clarified and theoretically explained.

Both CaF_2 and BaF_2 are typical F^- ion conductors with the fluorite structure. The mechanism of ion diffusion in the compounds with fluorite structure has been clarified in more detail than in other ionic conductors [8–10]. The purposes of the present investigation are (i) to confirm the possibility of acceleration of ionic conduction in the anionic conductors by dispersion of Al_2O_3 particles and (ii) to estimate the effective thickness and the conductivity of the interface layer in terms of a simple matrix-particle mixing model.

2. Experimental procedure

As starting materials, CaF_2 (99.99%, Rare Metallic

0022–2461/85 $03.00 + .12

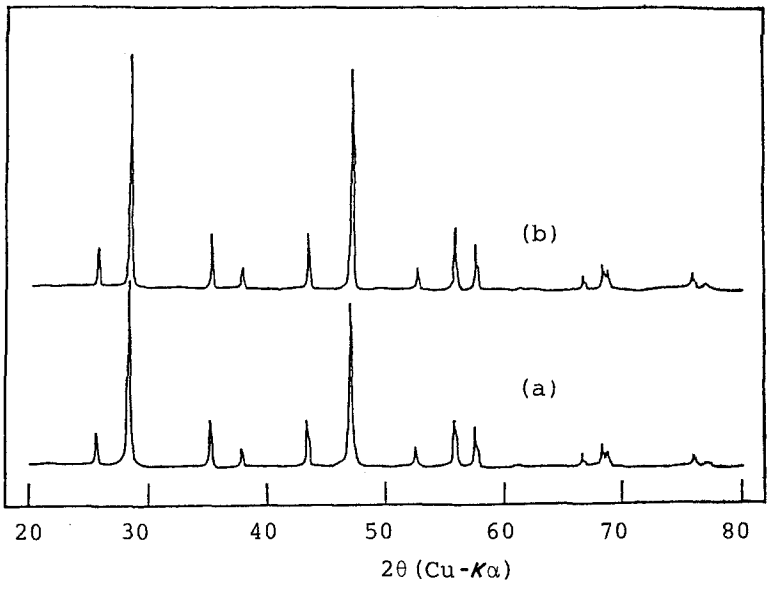

Figure 1 The X-ray diffraction patterns for (a) pre-heated and (b) post-heated $50CaF_2-50Al_2O_3$.

Co., Ltd), $Ba(NO_3)_2$ (99.9%, Hikotaro Shuzui Co., Ltd), NH_4F (99.9%, Kanto Chemical Co., Inc.) and Al_2O_3 (99.9%) of different reported particle sizes (0.06, 0.3, 8 μm, Marumoto Kogyo Co., Ltd) were employed. Alumina particles usually were aggregated to form larger secondary particles in the sample preparation process, so that the average particle size was measured by the sedimentation method. The measurement showed that 0.3 and 8 μm Al_2O_3 particles aggregated into secondary particles of 2.6 and 8.2 μm, respectively. The samples for measurements were prepared by the methods mentioned below.

2.1. $CaF_2-Al_2O_3$

The starting powders of CaF_2 and Al_2O_3 were vacuum dried at 400 and 600° C, respectively for at least 4 h prior to use. Appropriate amounts of CaF_2 and Al_2O_3 were dispersed in acetone and intimately mixed in an agate mortar until the acetone evaporated completely. The obtained powder was pelletized under a pressure of 200 to 300 MPa in a steel die and sintered at 900° C for 4 h in vacuum.

2.2. $BaF_2-Al_2O_3$

The aqueous solution of NH_4F was poured into that of $Ba(NO_3)_2$ containing dispersed alumina particles, so that the precipitates of BaF_2 could surround the Al_2O_3 particles. The mixture of BaF_2 and Al_2O_3 was dried at 120° C for 12 h in an oven and vacuum dried at 500° C for 4 h. The powders were pelletized by a method similar to that given in Section 2.1, and sintered at 800° C for 4 h in vacuum.

2.3. X-ray diffraction and microstructure observation

X-ray diffraction patterns of the pre-heated and post-heated samples were measured at room temperature using Cu$K\alpha$ radiation and a nickel filter (Rotaflex RU-200, Rigaku Denki Corp.).

The microstructure of the polished surface coated with carbon by vacuum evaporation and characteristic X-ray images of the elements were observed in the EPMA system (Hitachi, X-650)

2.4. Electrical conductivity

The two polished faces of the sintered sample were coated with sputtered Pt–Pd films which were used as blocking electrodes. The impedance was measured by an impedance analyser (HP-4192A) at 300 to 600° C in dry N_2. The impedance of the sample which was obtained by excluding the impedance resulting from the blocking electrodes, was adopted from the complex impedance plots obtained at 5 Hz to 10 MHz.

3. Results and discussion

3.1. Enhancement of ionic conduction and the formation of the interface layer

As is shown in Fig. 1, no difference can be seen in the X-ray diffraction patterns between pre-heated and post-heated mixtures of CaF_2 and Al_2O_3, indicating that the heat treatment merely affected densification of the mixture without

an accompanying chemical reaction or solid solution formation, as long as the heating temperature was below 1000° C. This was also the case for the BaF_2 and Al_2O_3 mixture. However, the samples heated above 1000° C contained $CaAl_2O_4$ or $BaAl_2O_4$ and other unknown phases as their reaction products.

A scanning electron micrograph of the microstructure of $80CaF_2$–$20Al_2O_3$ sintered at 900° C and characteristic X-ray images of the same area are shown in Fig. 2. It is seen that the aluminium-rich phases are dispersed in a matrix of a calcium-rich phase. These microstructural observations along with the above X-ray diffraction analysis were thought to confirm that the dispersed Al_2O_3 particles were surrounded by the CaF_2 matrix with no other X-ray detectable phases.

The composition and the particle size dependences of the electrical conductivity for the CaF_2–Al_2O_3 system obtained at 500° C are shown in Fig. 3. The electrical conductivity increases initially, goes through a maximum, and then decreases with increasing content of the dispersed Al_2O_3 in all cases, with the Al_2O_3 concentration giving the maximum conductivity increases with an increase in the starting particle size of Al_2O_3.

Explanation for the composition and particle size dependences of the conductivity may be possible when one assumes that certain highly ionic conductive interfaces between the conductor matrix and Al_2O_3 particles are formed. This concept was already proposed for the Al_2O_3 dispersed system of LiI [1], CuCl [6] and AgI [7]. According to Jow and Wagner [6], the interface region may possess different concentrations of lattice defects than in the interior of the matrix phase far from the interface and can hence be regarded as a space charge region having certain effective thickness. Thus the interface region with effective thickness will be called the "interface layer" hereafter. If the thickness of the interface layer is independent of the particle size of Al_2O_3, the total volume of the interface layers is larger in a sample with finer Al_2O_3 particles at some fixed composition and thus gives rise to a higher ionic conductivity. As shown in Fig. 3

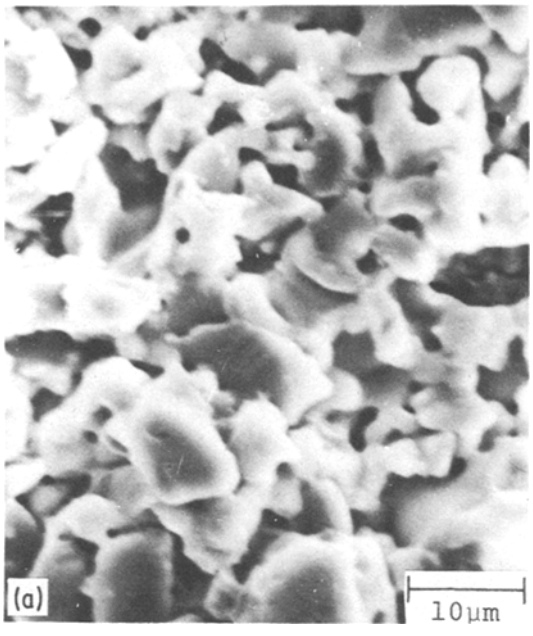

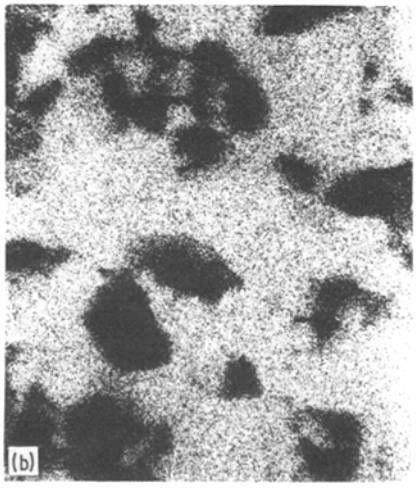

Figure 2 Scanning electron micrograph for $80CaF_2$–$20Al_2O_3$ (a) and the X-ray images of the same area for (b) Ca$K\alpha$ and (c) Al$K\alpha$. 8 μm Al_2O_3 was used in this sample.

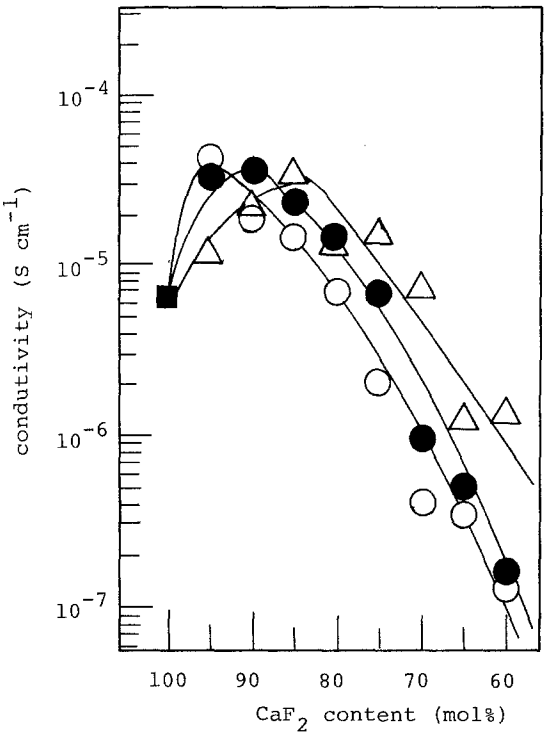

Figure 3 Composition and Al_2O_3 particle size dependences of the electrical conductivity at 500° C for the system CaF_2–Al_2O_3. ○ – 0.06 μm Al_2O_3; • – 0.3 μm Al_2O_3; △ – 8 μm Al_2O_3.

the conductivity of $95CaF_2$–$5Al_2O_3$ increases with decreasing Al_2O_3 particle size, which supports this assumption.

In so far as the concentration of Al_2O_3 is low and all the particles are completely surrounded by the matrix conductor phase as shown in Fig. 4a, the total conductivity of the system would increase with increasing concentration of Al_2O_3. When the total volume of the interface layers formed becomes the largest or the interface layers are most effectively linked together as shown in Fig. 4b, the sample would show maximum conductivity. As the concentration of Al_2O_3 further increases, the number of Al_2O_3 particles which are not completely covered by the interface layers would become smaller as shown in Fig. 4c and the total conductivity would decrease. These considerations could qualitatively explain the composition dependence of the conductivity shown in Fig. 3. They also give us a clue towards elucidating the dependence of maximum conductivity on the particle size of Al_2O_3; the amount of the matrix phase to form interface layers must be larger for finer Al_2O_3 particles due to their larger specific surface area, which would lead to the tendency that the concentration of Al_2O_3 to give maximum conductivity increases with increasing particle size as was experimentally confirmed.

Fig. 5 shows the variation of the conductivity (at 500° C) of the $80CaF_2$–$20Al_2O_3$ as a function of the calcining temperature, showing that the interface layers are most effectively formed at 900° C in vacuum and also that the reaction

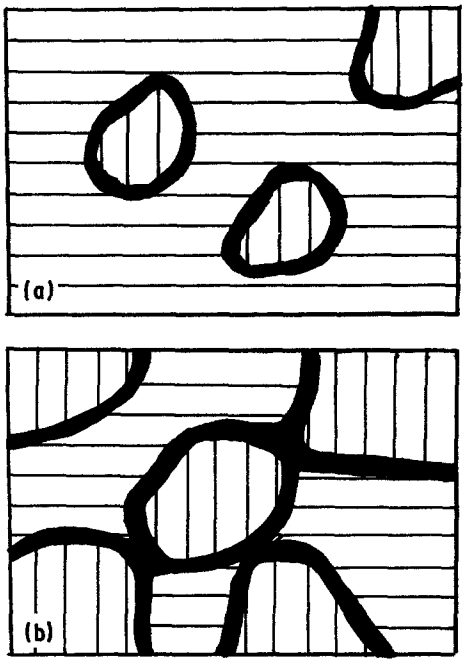

Figure 4 A model for explaining the particle size and composition dependences of the conductivity. (a) A small amount of Al_2O_3 particles separately dispersed in the matrix. (b) Interface layers contacting and forming highly conductive paths. (c) Large quantity of additional Al_2O_3 and the existence of the Al_2O_3 particles not surrounded by the interface layer. ≡ – matrix; ||| – particle; ∽ –interface

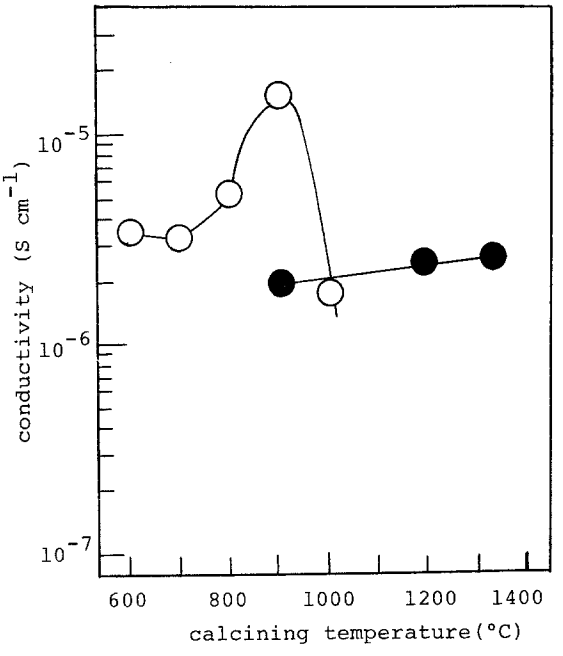

Figure 5 Electrical conductivity at 500° C for the system $80CaF_2$–$20Al_2O_3$ (0.3 μm Al_2O_3 used) obtained by varying the calcining temperature. ○ – calcined in vacuum; ● – calcined in air.

products formed above 1000° C do not contribute to the enhancement of ionic conduction.

3.2. Estimation of the thickness and the conductivity of an interface layer

Jow and Wagner [6] theoretically treated the enhancement of ionic conduction by Al_2O_3 dispersion in the system CuCl–Al_2O_3. They adopted the assumption that a pure ionic crystal in thermal equilibrium possessed a space charge region adjacent to the surface formed due to the difference in free energies of formation among different defect species [11–13]. They extended this assumption to the interface between a conductor matrix and an Al_2O_3 particle, in which the excess conductivity due to the addition of Al_2O_3 was expressed as

$$\Delta\sigma \cong \sum_i e\mu_i \Delta n_i \lambda (1/r_1)[V_v/(1 - V_v)] \quad (1)$$

where e is the electronic charge, μ_i the mobility of the ith defect species and Δn_i is the average excess defect concentration in the space charge region with an effective thickness λ, and r_1 and V_v are the average radius and the volume fraction of Al_2O_3 particles, respectively. Equation 1 is only applicable to the system where r_1 is small enough when compared to the average distance of the two nearest Al_2O_3 particles. At a definite temperature, the excess conductivity, $\Delta\sigma$, is proportional to $(1/r_1)[V_v/(1 - V_v)]$. The excess conductivity should be inversely proportional to the alumina particle size, if the particles are approximately spherical and of uniform size. This has been verified for the system LiI–Al_2O_3, CuCl–Al_2O_3 and AgI–Al_2O_3. The thickness, λ, of a space charge layer is

$$\lambda = \left[\frac{8\pi e^2}{\epsilon kT} n_v(\infty)\right]^{-1/2} = \left[\frac{8\pi e^2}{\epsilon kT} n_i(\infty)\right]^{-1/2} \quad (2)$$

where ϵ is the static dielectric constant. The symbols, $n_v(\infty)$ and $n_i(\infty)$ are the equilibrium defect concentrations of vacancies and interstitial ions in the interior of the matrix conductor phase. The calculated thickness for the system CuCl–Al_2O_3 was reported to be 150 nm [14]. For the system BaF_2–Al_2O_3, the proportional relationship between the conductivity and $(1/r_1)[V_v/(1 - V_v)]$ was recognized in the composition range where enhancement of ionic conduction was observed. However, λ could not be calculated because of the impossibility of the estimation of ϵ and $n_v(\infty)$.

Stoneham *et al.* [3] extended Landauer's effective medium model [4] for the system LiI–Al_2O_3, successfully explaining the composition dependence of the conductivity.

In this work, the conductivity and the thickness of the highly conductive interface layer formed between BaF_2 and Al_2O_3 were calculated using another method. To obtain adequate results, the sample had to be prepared to satisfy the condition of the ideal model as shown in Fig. 6. The model consists of the spherical dispersoid (Al_2O_3) and matrix phase (BaF_2) without pores and the dispersoid is surrounded by the interface layer with high ionic conductivity. To realize this condition, the particle must have ideal wettability to the matrix. However, an ideal dispersion of Al_2O_3 particles could not be attained, since the reaction between BaF_2 and Al_2O_3 took place above the melting point of BaF_2 (1368° C). In order to prepare the system close to the ideal condition, the method mentioned in Section 2.2 was applied. In the CaF_2–Al_2O_3 system, the precipitates were not filtered successfully because they were too fine.

Maxwell [15] proposed the equation for the total conductivity of the system as shown in Fig. 6:

$$\sigma = \sigma_1 \frac{\sigma_1 + 2\sigma_2 + 2\nu_2(\sigma_1 - \sigma_2)}{\sigma_1 + 2\sigma_2 - \nu_2(\sigma_1 - \sigma_2)} \quad (3)$$

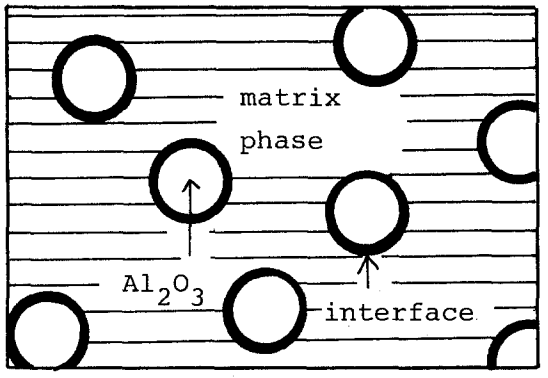

Figure 6 The ideal dispersion model to which Maxwell's equation is applicable. The particles are surrounded by the matrix phase with no pores.

where σ_1 is the conductivity of a particle, σ_2 is the conductivity of a matrix and ν_2 is the volume fraction of the matrix. In the present calculation, the conductivity of BaF_2 single crystal, 10^{-6} S cm^{-1}, was used for σ_2 and ν_2 was approximated as the volume fraction of BaF_2 at the starting composition. The measured total conductivity and the calculated conductivity of a particle are shown in Fig. 7. The conductivity of a particle, σ_1, seems to be too high when compared with that of a pure alumina particle and hence it should be considered that σ_1 is composed of the conductivity of an interface layer and that of an alumina particle, the model of which is shown in Fig. 8.

The conductivity of the particle shown in Fig. 8 can be calculated by the following equation [16]:

$$\sigma_{\text{eff}} = \sigma_b \frac{R_2^3(\sigma_a + 2\sigma_b) + 2R_1^3(\sigma_b - \sigma_a)}{R_2^3(\sigma_a + 2\sigma_b) + R_1^3(\sigma_b - \sigma_a)} \quad (4)$$

where σ_{eff} is the total conductivity of the particle which corresponds to σ_1 in Equation 3 and the other parameters have the meanings as shown in Fig. 8. As already mentioned, the alumina powders aggregated into larger secondary particles, such that the half of the secondary particle size was put into R_1 in Equation 4. It was considered that the conductivity of the interface layer, σ_b, was large enough to neglect that of Al_2O_3, σ_a. Consequently, the relation between the thickness $(R_2 - R_1)$ and the conductivity of an interface layer were calculated by Equation 4 and are shown in Fig. 9. If both conductivity and thickness are independent of the composition and the particle size of Al_2O_3, the crossing point of

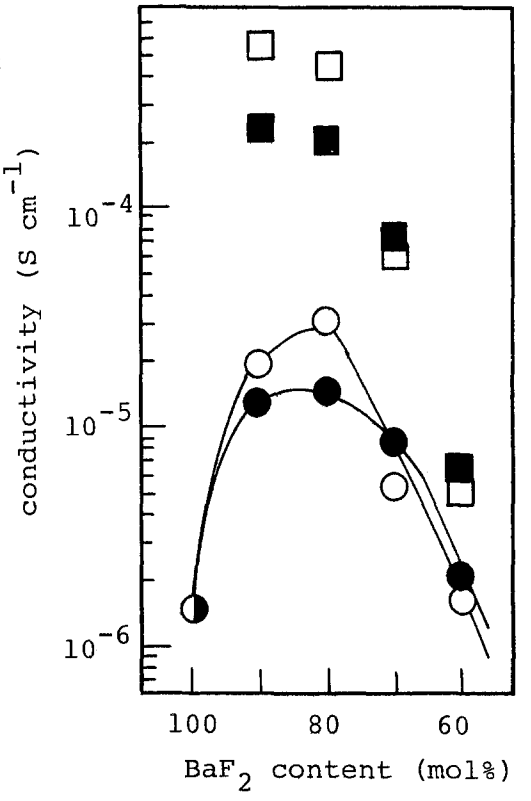

Figure 7 The electrical conductivity of the system BaF_2–Al_2O_3 and the calculated conductivity of the particles at 500° C. ■ – calculated conductivity of the particle with 8 μm Al_2O_3; □ – calculated conductivity of the particle with 0.3 μm Al_2O_3; • – measured conductivity with 8 μm Al_2O_3; ○ – measured conductivity with 0.3 μm Al_2O_3.

the dashed and solid curves would give the thickness and the conductivity of the interface layer in the BaF_2–Al_2O_3 system. From Fig. 9, it is estimated that the thickness is 0.3 to ~ 0.6 μm and the conductivity is about 10^{-3} S cm^{-1} at 500° C. The conductivity of an interface layer is ~ 3 orders of magnitude larger than that of a

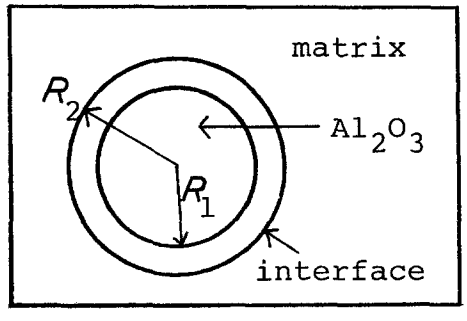

Figure 8 A model for the Al_2O_3 particle covered with an interface layer.

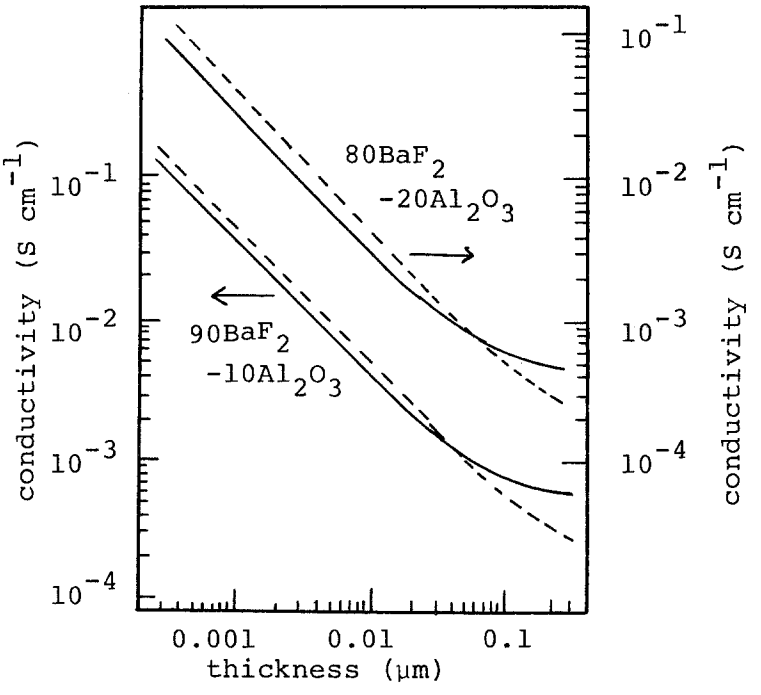

Figure 9 The relation between the conductivity and the thickness of the interface layer. The crossing point of the solid (2.6 μm Al_2O_3 system) and dashed (8.2 μm Al_2O_3 system) curves gives the conductivity and the thickness of the interface layer.

bulk single crystal BaF_2, while its thickness is comparable to that obtained for the CuCl–Al_2O_3 system.

4. Summary

Enhancement of the ionic conductivity by the dispersion of Al_2O_3 particles was confirmed in the systems CaF_2–Al_2O_3 and BaF_2–Al_2O_3. The interface layer between the conductor matrix and the insulator particles contributes to this phenomenon and the existence of the interface layer was explained on the basis of the particle size and composition dependences of the conductivity. The conductivity and the thickness of the interface layer were estimated by using the simple mixing model: the conductivity of the particle surrounded by the interface layer in the matrix phase was calculated by Maxwell's equation and the relation between the conductivity and the thickness of the interface layer was obtained by the Tiku–Kröger equation. Based on the assumption that the conductivity and the thickness of the interface layer were independent of both Al_2O_3 particle size and composition, they were estimated to be $\sim 10^{-3}$ S cm^{-1} and 0.3 to 0.6 μm, respectively, at 500° C.

Acknowledgement

The authors wish to thank Dr Masayuki Nagai, Musashi Institute of Technology, for helpful discussions. This work was partially supported by a Grant-in-Aid for Scientific Research from the Japanese Ministry of Education, Science and Culture (No. 58470054)

References

1. C. C. LIANG, *J. Electrochem. Soc.* **120** (1973) 1289.
2. *Idem, ibid.* **123** (1976) 453.
3. A. M. STONEHAM, E. WADE and J. A. KILNER, *Mater. Res. Bull.* **19** (1979) 661.
4. R. LANDAUER, *Rev. Mod. Phys.* **45** (1973) 574.
5. S. PACK, B. OWENS and J. B. WAGNER JR, *J. Electrochem. Soc.* **127** (1980) 2177.
6. T. JOW and J. B. WAGNER Jr, *ibid.* **126** (1979) 1963.
7. K. SHAHI and J. B. WAGNER Jr, *ibid.* **128** (1981) 6.
8. E. BARSIS and A. TAYLOR, *J. Chem. Phys.* **48** (1968) 4357.
9. *Idem, ibid.* **45** (1966) 1154.
10. P. VAROTSOS and K. ALEXOPOULOS, *J. Phys. Chem. Solids*, **42** (1981) 409.
11. K. LEHOVEC, *J. Chem. Phys.* **21** (1953) 1123.
12. K. L. KLIEWER and J. S. KOEHLER, *Phys. Rev. A* **140** (1965) 1226.
13. K. L. KLIEWER, *J. Phys. Chem. Solids* **27** (1966) 705.
14. J. B. WAGNER Jr, private communication (1983).
15. J. C. MAXWELL, "Electricity and Magnetism", Vol. 1, 3rd edn (Heywood, London, 1965) p. 440.
16. S. K. TIKU and F. A. KRÖGER, *J. Amer. Ceram. Soc.* **63** (1980) 183.

Received 9 April
and accepted 31 July 1984